

Chaotic itinerancy in a coupled-element multistable optical chain

Kenju Otsuka

NTT Basic Research Laboratories, Musashino-shi, Tokyo, 180 Japan

(Received 15 August 1990)

Self-induced wandering among local attractors, that is, *chaotic itinerancy*, and the chaotic search of coexisting periodic or chaotic local orbits have been discovered in a nonequilibrium optical system with distributed nonlinear elements (Otsuka-Ikeda model system). It is shown on the basis of numerical simulations that spatiotemporal chaos in this system is interpreted as unstable motions which dynamically connect destabilized spatial structures via a chaotic itinerancy process.

Spatiotemporal dynamics in high-dimensional nonequilibrium systems are important current issues in nonlinear physics. In general, such systems possess coexisting equilibria as stationary solutions. The motivation of our recent studies is to extract generic phenomena from such multiequilibria systems, paying special attention to the dynamics appearing when coexisting equilibria become dynamically unstable. With this motivation, we have investigated this general issue for years, and recently discovered a self-induced switching between local equilibria resulting from chaotic motions created within themselves, i.e., chaotic itinerancy, in some high-dimensional chaotic systems including coupled laser systems,¹ multimode Maxwell-Bloch equations,² and complex time-dependent Ginzburg-Landau (TDGL) systems.³ The nonlinearity responsible for the self-induced escape from the local attractors changes from one system to another. However, local chaos self-created within the local attractor, which is closely correlated with the past evolution (*memory*) of the system, commonly plays an inevitable role in chaotic itinerancy phenomena. Indeed, when realizing an escape from a local attractor by an externally applied random force in these systems, the local attractor is severely damaged, resulting in a complete blackout of memory.

The purpose of this Rapid Communication is to present another example of chaotic itinerancy, which is expected in the Otsuka-Ikeda bistable chain model.^{4,5} In the above-mentioned systems which exhibit chaotic itinerancy, however, coexisting equilibria can be defined by simple successive winding numbers easily determined by boundary conditions. In addition, self-induced switching has been found to take place only between adjacent winding-number states having similar basins of attraction. In short, chaotic itinerancy occurs in these systems in the form of a simple successive topological change to an adjacent winding-number state. On the other hand, the Otsuka-Ikeda model system ensures the existence of a variety of local attractors which possess different characters and cannot be expressed by winding numbers, resulting from its inherent multistable nature. Therefore, the spatiotemporal dynamics connecting these attractors is expected to show richer features than seen in previous systems.

In the Otsuka-Ikeda model shown in Fig. 1, nonlinear

refractive index elements are arranged in an optical ring cavity and individual elements are coupled via counterpropagating light beams (A_F and A_B) that are introduced through the mirrors which separate the elements. If we neglect the refractive-index grating effect due to interference and assume lossless media, then the dynamics of the two fields $E_F^{(k)}$ and $E_B^{(k)}$ are governed by the following simple equations, within the limit of large dissipation:^{4,5}

$$\begin{aligned} \tau \dot{\phi}_k &= -\phi_k + f_F(\phi_{k-1}) + f_B(\phi_{k+1}) \\ &\equiv -\phi_k + |E_F^{(k)}|^2 + |E_B^{(k)}|^2, \end{aligned} \quad (1)$$

$$f_{F,B}(\phi_k) \equiv A_{F,B}^2 [1 + 2B \cos(\phi_k + \phi_0)]. \quad (2)$$

Here, ϕ_k is the nonlinear phase shift, ϕ_0 is the linear phase shift, B is the coupling coefficient between the adjacent cells, and τ is the medium response time.

Let us briefly summarize spatial patterns created in this system.⁵ When input intensity $A_{F,B}^2$ is small, a variety of spatial heteroclinic structures born from stable period-two cycle fixed points are realized as dynamically stable equilibria. As the input intensity is increased up to the

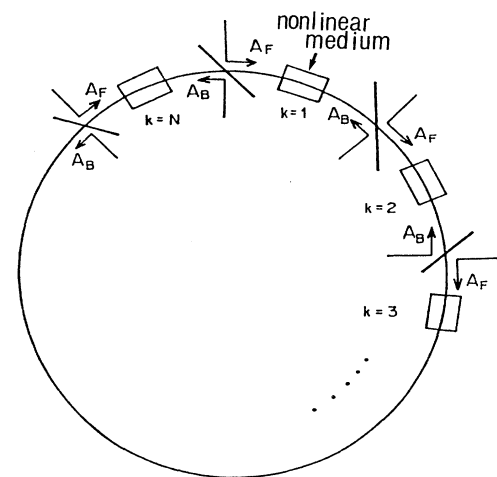


FIG. 1. Conceptual model of a multistable optical chain with coupled nonlinear elements. (Otsuka-Ikeda model system.)

multistable domain, interheteroclinic structures, which connect different coexisting period-two cycle solutions, as well as chaotic patterns, which make rounds between an extremely large variety of different fundamental periodic structures, exist stably in time. These coexisting spatial patterns are categorized into several classes in terms of the norm from the period-two cycle solutions. Needless to say, the number of coexisting patterns increases with input intensity $P = A_A^2 + A_B^2$ as well as with system size N . When P is increased further, these patterns become dynamically unstable and spatiotemporal chaos (STC) develops.

The question then arises: *What kind of spatiotemporal dynamics takes place in the process where these coexisting patterns become dynamically unstable and develop into STC?* The main issue of this study is to provide an answer to this question. From extensive numerical simulations, the following scenario has been found to exist when P is increased. Some of the stable chaotic spatial patterns become dynamically unstable and exhibit periodic pulsations, reflecting the different dynamical stability of each pattern. The number of destabilized patterns increases with P . In some cases, periodic pulsations come to be modulated by intermittent bursts and lead to chaotic pulsations around local attractors as P is smoothly increased, resulting in local chaos, while some local chaotic

orbits often appear suddenly. (A detailed characterization of local chaos by power-spectrum analyses is now under investigation.) This implies that a variety of stable fixed points, periodic, quasiperiodic orbits as well as chaotic orbits belonging to different attractors (spatial patterns) coexist at fixed P values. Which state is realized during the course of temporal evolution critically depends on the initial values of each element.

Figures 2 and 3 show typical examples of temporal evolutions of ϕ_k for different initial values, where $N=9$, $B=0.3$, and $\phi_0=0$ are assumed. In these simulations, the system is initially set on the same orbit and then perturbations of different strengths are applied in the form of trigger pulses to ϕ_0 . In Fig. 2, the norm from the fundamental period-two cycle solution,

$$D \equiv \left[\sum_{k=1}^N |\cos(\phi_k) - \cos(\phi_{k-2})|^2 \right]^{1/2},$$

is plotted to classify and distinguish periodic patterns. Note that periodic patterns (a) and (b) have the same time-averaged norm, as also do (c) and (d).

In Fig. 3, the temporal evolution of the local Lyapunov

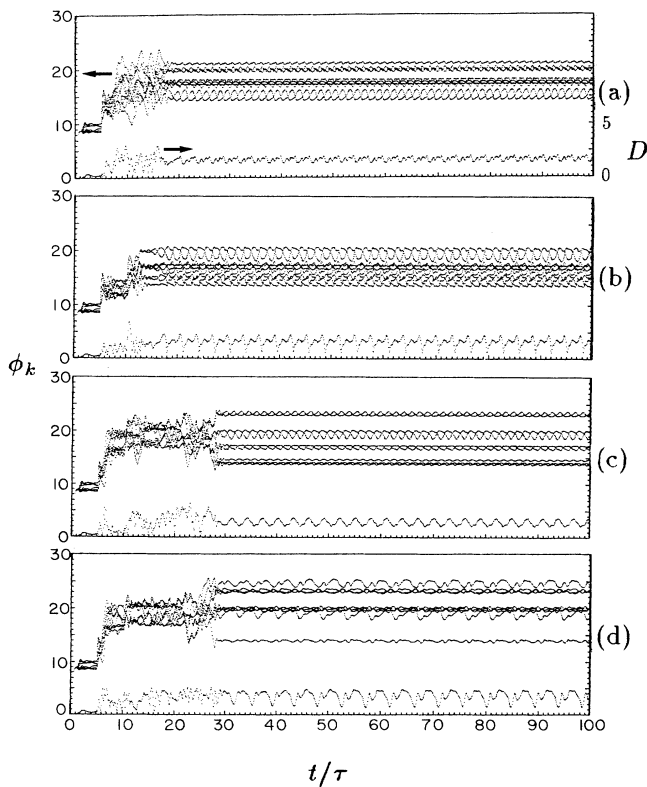


FIG. 2. Chaotic search of periodic orbits for different initial conditions. $N=9$, $B=0.3$, $P=18$, and $\phi_0=0$. Trigger pulses are applied in the period $5 < t/\tau < 10$ to ϕ_0 of all cells. D is the norm from the fundamental period-two cycle pattern.

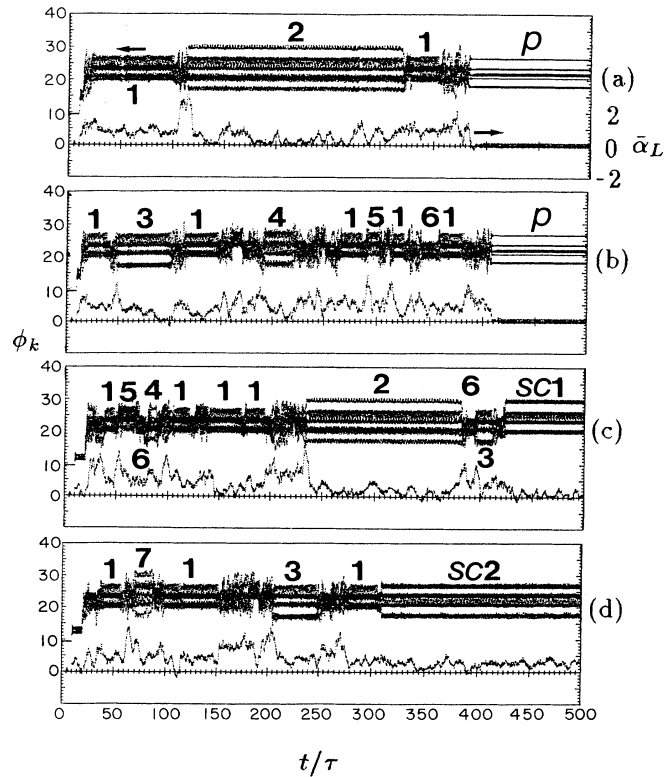


FIG. 3. Chaotic itinerancy in high- P regimes for different initial conditions. $P=23$ and other adopted parameters are the same as those of Fig. 2. Trigger pulses are applied in the period $10 < t/\tau < 20$. ρ denotes a periodic orbit and SC means stable local chaos, where different unstable chaotic orbits are distinguished by numbers. $\bar{\alpha}_L$ is the time-averaged local Lyapunov exponent.

exponent defined as

$$\alpha_L(t) \equiv \frac{1}{2} \ln \sum_{k=1}^N \delta\phi_k(t)^2, \quad (3)$$

averaged over $\Delta t/\tau=5$ is also shown. Here, $\delta\phi_k(t)$ is calculated by the variational equation

$$\tau\delta\dot{\phi}_k = -\delta\phi_k + f'_F(\phi_{k-1})\delta\phi_{k-1} + f'_B(\phi_{k+1})\delta\phi_{k+1}. \quad (4)$$

This quantity denotes the measure of stability of each pattern. When P is relatively low as in the case of Fig. 2 ($P=18$), there are many coexisting periodic orbits in phase space. After some transients, the system is attracted by one of the coexisting periodic orbits whose long-time average of local Lyapunov exponents is zero, depending on initial conditions. As P is increased, some of these periodic orbits are chaoticized and turn out to be local chaotic orbits. In these regimes, as shown in Fig. 3 ($P=23$), the system exhibits self-induced switching among different *unstable* local chaotic orbits indicated by numbers, i.e., chaotic itinerancy, and finally finds one of the periodic (like p in Fig. 3) or *stable* chaotic orbits (SC1 and SC2), from which the system cannot escape. There are other coexisting orbits, although they are not shown in Fig. 3. The stable local chaotic orbits mean that the system cannot escape from these orbits eternally, resulting in local chaos. Note that Lyapunov exponents for these stable local chaotic attractors are smaller than those for unstable ones in which the system cannot stay for a long time as can be seen in Fig. 3(c) and 3(d). This implies that there exists a threshold $\bar{\alpha}_{L,th}$ for the system to escape from the local chaotic attractors. If one increases P further, the system can hardly find periodic or stable local chaotic orbits and chaotic itinerancy persists and leads to global STC. This strongly suggests that STC in the present system is interpreted as unstable motions which dynamically connect destabilized spatial structures via a chaotic itinerancy process. As the system size N increases, the number of local attractors, among which chaotic itinerancy takes place, increases. In addition, it should be noted that dwell time within the local attractor decreases with the increase in local Lyapunov exponent in a chaotic itinerancy regime as shown in Fig. 3. This tendency has been confirmed by a statistical analysis of numerous experimental data. As P is increased, local Lyapunov exponents become to distribute at higher values and results in the decrease in dwell times within unstable local chaotic attractors.

What is the origin of the self-induced switching among different local attractors? This is the key for understanding chaotic itinerancy in this system. To investigate this problem, we calculate the evolutions of field intensities $|E_k|^2 \equiv |E_F^{(k)}|^2 + |E_B^{(k)}|^2$ which provide the on-site nonlinearity giving rise to nonlinear phase rotation. This quantity expresses the phase rotation speed of individual elements, as is seen from Eq. (1). A typical example near the switching point of Fig. 3(a) is depicted in Fig. 4. It is apparent from the figure that the electric field of k =fourth cell, i.e., $|E_4|^2$ decreases at first (see point a in the figure) and this information is transferred to adjacent cells successively as shown by arrows, due to the mutual coupling between adjacent cells. As a result, all the cells

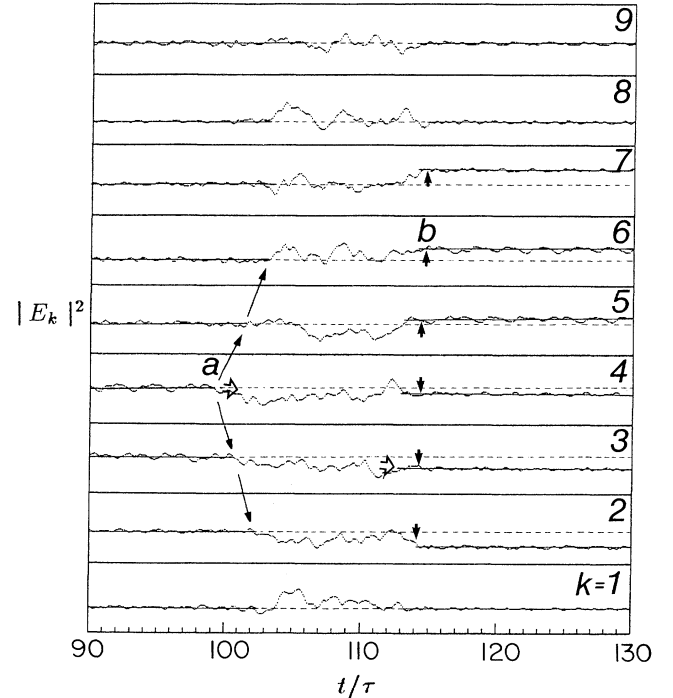


FIG. 4. Temporal evolutions of field intensities for cells near the switching point of Fig. 3(a) ($90 < t/\tau < 130$).

cooperatively escape from the local attractor 1. When state values of the majority of the cells enter the basin of a new attractor, the system switches to this attractor and the self-induced switching to local attractor 2 is established at point b . It should be noted that, in the case of Fig. 4, $k=1, 8,$ and 9 cells are fluctuating around the same state values even after the switching, while other cells fluctuate around different state values. This results from the fact that switching will take place favorably between structures that are nearby in terms of the norm, where some of the cells have the same state values. In such cases, successful switching can be attained by changing the spatial structures *locally*. However, a switching path is not unique in the present system, as shown in Fig. 3. This is a sharp contrast to the previous itinerant systems in which chaotic itinerancy always take place between adjacent winding-number states and the easy path for switching is uniquely established. The connectivity between different attractors,⁵ which may depend on the norm between spatial patterns, and the identification of switching paths of chaotic itinerancy in the present system are interesting problems for future study.

In conclusion, chaotic itinerancy among coexisting local attractors has been discovered in a multistable optical system which possesses a variety of spatial patterns. The creation of field inhomogeneity and a cooperative phase rotation are found to be the origin of the self-induced switching according to numerical simulations. This mechanism is very similar to that for chaotic itinerancy in weakly coupled complex TDGL systems,³ although different switching paths exist in the system discussed in this paper.

Fruitful discussions with K. Ikeda are acknowledged.

¹K. Otsuka, Phys. Rev. Lett. **65**, 329 (1990).

²K. Ikeda, K. Otsuka, and K. Matsumoto, Prog. Theor. Phys. **99**, 295 (1989).

³K. Otsuka and K. Ikeda, in *Proceedings of OSA Topical Meeting on Nonlinear Dynamics in Optical Systems, Afton, 1990*,

edited by N. B. Abraham, E. Garmire, and P. Mandel (Optical Society of America, Washington, DC, 1990); K. Otsuka, Int. J. Mod. Phys. B (to be published).

⁴K. Otsuka and K. Ikeda, Phys. Rev. Lett. **59**, 194 (1987).

⁵K. Otsuka and K. Ikeda, Phys. Rev. A **39**, 5209 (1989).